# Air Jet Erosion studies on Aluminum - Red Mud Composites using Taguchi Design.

Anil K C
Dept. of Industrial Engineering and Management, Siddaganga Institute of Technology

Kumaraswamy
Dept. of Mechanical Engineering, R L Jallapa Institute of Technology

Reddy, Mahadeva
Dept. of Mechanical Engineering, Jayawantrao Swant College of Engineering

Mamatha K M
Dept. of Mechanical Engineering, Mangalore Institute of Engineering and Technology

https://doi.org/10.5109/6781059

出版情報：Evergreen. 10 (1), pp.130-138, 2023-03. 九州大学グリーンテクノロジー研究教育センター
バージョン：

# Air Jet Erosion studies on Aluminum - Red Mud Composites using Taguchi Design.

Anil K C[1*], Kumaraswamy[2], Mahadeva Reddy[3], Mamatha K M[4]

[1]Dept. of Industrial Engineering and Management, Siddaganga Institute of Technology, Karnataka, India.

[2]Dept. of Mechanical Engineering. R L Jallapa Institute of Technology, Doddaballapura, Karnataka, India.

[3]Dept. of Mechanical Engineering. Jayawantrao Swant college of Engineering, Pune, India

[4]Dept. of Mechanical Engineering. Mangalore Institute of Engineering and Technology, Mangalore, India

E-mail: anilkc@sit.ac.in

(Received December 2, 2022; Revised January 19, 2023; accepted January 23, 2023).

**Abstract**: Due to its numerous uses in the industries of aerospace, defense, automotive, and marine, among others, metal matrix composites (MMCs) are currently receiving a lot of attention in the world of materials., the present work focuses on characteristics of erosive behaviour of Al-Red mud (Rm) reinforced composites developed by stir casting and the effect of red mud in the aluminum metal matrix composites in composition of 2% wt., 4% wt., 6% wt., 8% wt. which is subjected to various tests to study their wear properties in comparison to base alloy. Experiments are conducted under laboratory conditions to assess the air jet erosion characteristics of the red mud reinforced aluminum composites according to ASTM G76 standard. Finally, the surface of the worn-out sample is studied under the Scanning Electron Microscope, to get an idea about the effect of red mud reinforcement on erosion behaviour of the composite. The collected data was analyzed and visualized in Minitab V19 software. To find SN plots, Taguchi analysis was performed on the collected data. ANOVA and regression analysis were both used to determine the associations between the many parameters that were chosen. Form the overall analysis Al- composites consist 8% of RMp shows the optimum erosion at SOD of 30mm at 15 and 90 degree of impact angle for 3mins of time.

Keywords: Al-8011 alloy; Red mud; Taguchi; ANOVA; Air jet erosion

## 1. Introduction

The ability of civilization to generate and manufacture materials to suit the requirements of its people has been inextricably tied to its advancement. Materials' characteristics are determined by both their structure and content. Metals are the most reactive of the three materials, meaning they react quickly with other substances. Ceramics are the least reactive, meaning they react slowly with other substances. Polymers are the most stable of the three materials, meaning they resist breaking down or reacting with other substances. When it comes to getting the correct balance of toughness, strength, stiffness, and density, traditional materials are constrained [1-5, 27-31]. Composites are the most promising materials of interest for overcoming these drawbacks and meeting the demands of modern technology. When compared to non-abrasive alloys, The characteristics of MMCs, such as their high specific strength, specific modulus, damping capacity, and excellent wear resistance, are greatly increased. Composites with low densities and low costs are becoming more popular. The periodic table contains 118 elements, of which 95 are metals. Due to the absence of widely accepted definitions for the categories involved, the boundaries between metals, nonmetals, and metalloids vary slightly, making the number imprecise. Ceramics are inorganic non-metallic materials made up of metallic and non-metallic components held together by ions and covalent bonds [6-9]. Ceramics are made from a variety of materials, but all major engineering ceramics are crystalline. This is because crystalline materials have a very regular structure that makes them strong and durable. Because there are no conducted electrons in ceramics, they are good electrical and thermal insulators. It also has high melting temperature and chemical stability in various unfavorable situations due to its strong connection strength [10]. The plastic flow of metal is mainly caused by slides. This is because metals have no directionality of metal bonds, so the alternation moves with relatively low stress and, all atoms involved have a uniformly distributed negative charge on the bonding surface. The metal bonding process does not involve positively or negatively charged ions. Ceramics, on the other hand, form ionic or covalent connections that prevent dislocations and the slide from moving [11-15]. The difficulty of slip or alternate

motion is one of the causes for ceramics hardness and brittleness. Despite the fact that ceramics are inherently robust, in practice they do not fully exert their strength, as they cannot slip or bend into plastic to counteract even the smallest imperfections [16]. Until reaching the force of nature, they have prematurely brittle divisions. Since the bonds between atoms in covalently bonded ceramics are concrete and direct, electron charge exchange between atomic pairs is required. When sufficient stress is applied to the covalent decision, the separation of the electron pair bond causes a brittle fracture, eliminating the need for subsequent reformation [17-19]. Metal matrix composites (MMCs) and light metal matrix composites (LMCs) are used interchangeably by several researchers. Light metal matrix composites have made significant progress in recent decades, allowing them to be integrated into the most important applications. Depending on the application, the features of MMC can be combined into custom-made materials, bringing up a world of possibilities for modern materials science and development [20-26].

Aluminum matrix composites (AMCs) are materials made by combining aluminum with reinforcement materials such as ceramic particles, metal particles, or carbon fibers. These composites have a number of advantageous properties, including improved wear resistance. The wear resistance of AMCs is enhanced by the hard and abrasive reinforcement particles, which prevent the aluminum matrix from being worn away as easily. Additionally, the reinforcement particles can also improve the toughness and strength of the composite. The wear properties of AMCs can be further optimized by controlling the size and distribution of the reinforcement particles, as well as the bonding between the reinforcement and the aluminum matrix. Due to these properties, AMCs are finding increasing use in a variety of applications, including aerospace, automotive, and military industries.

In the light of the above, the present work focuses on characteristics of erosive behaviour of Al-RM reinforced composites developed by stir casting and the effect of addition of red mud in the aluminium metal matrix composites in composition of 2%Wt, 4%Wt, 6%Wt, 8%Wt which is subjected to various test parameters to study their wear properties in comparison to base alloy of Al-8011.

## 2. Materials & Fabrication

### 2.1 Aluminium-8011 alloy.

The matrix phase of the aluminum alloy is the subject of the majority of MMC research. It is encouraging to see the combination of ductility, lightness, corrosion resistance, environmental strength, and useful mechanical properties. The melting temperature is both high and low enough to accommodate a wide range of applications and processing techniques. Due of aluminum's ability to accommodate different reinforcements including particles, fibers, and whiskers. Because of their accessibility, affordable cost of manufacture, and comparatively isotropic features, the researcher has focused on AMCs. [4]. The aluminum alloys LM-25, 1100, 2024, 3014, 6061, 6063, 7072, 7075, and 8011 are the most often utilized ones in the manufacture of MMCs [1,2,3,6]. With the previously mentioned benefits, other qualities like being suitable for storing food and beverages, having high reflectivity, having good thermal and electrical conductivity, and being simple to recycle become very important. Al-8011 is an unclassified type of aluminum alloy. Compared to other Al-alloys, it possesses a high degree of ductility. Fe and Si are the primary alloying elements in Al-8011, which also contains significant amounts of tin and lithium [4]. Increasing density and the modulus of elastic aluminum alloys, the use of lithium-alloys as the primary structural material used in air-to-air heat exchangers [14], in the carry-over locks and connecting rods on diesel motor [14] is a good candidate for replacing the existing alloys in aerospace and defense applications [4] as well as the Al 8011 alloy. The aluminum 8011 series was selected as a matrix alloy. Heat treatability, high conductivity, strength, hardness, and typically good tensile strength are the main properties of the 8xxx series.

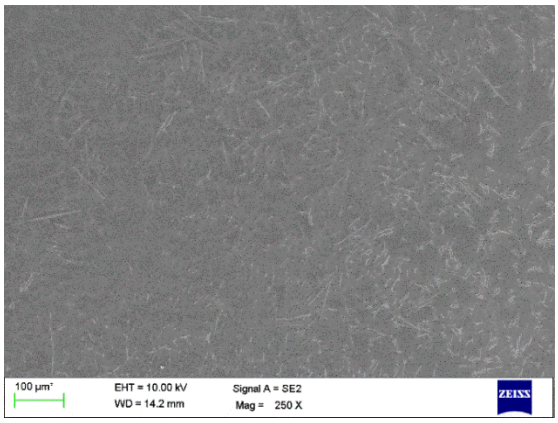


**Fig.1:** SEM image of Al-8011 alloy

Fe, Ni, and Li are among the frequently used alloying elements. The Al-8011 alloy is purchased from the Plas-met-chem. Corporation, Bangalore in the form of ingots. The SEM image of Al-8011 is shown in figure 1.

### 2.2 Red Mud.

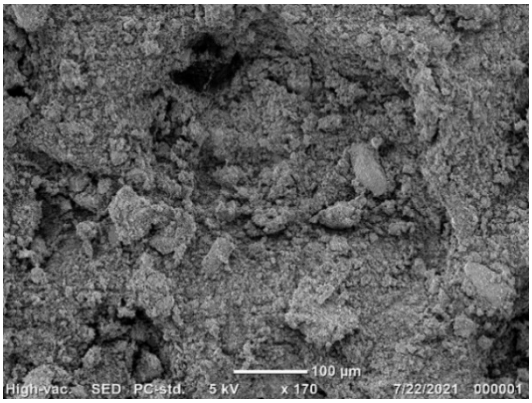


**Fig. 2:** SEM micrographs of red mud powder

From the late 19th century to date, aluminum refineries constantly produced the bauxite residue (Red Mud). It is one of the largest industrial by-products with a global level estimated at 25-40 billion tonnes at the end of 2017 [5].

As the inventory increases year after year, creating and implementing efficient storage and disposal programs is still crucial. Depending on the type of ore and the results of the Bayer process, the residue has different chemical and physical characteristics. Refineries face a significant problem in locating the best practices around the world to store bauxite residue and achieve minimal social and environmental impacts both during operation and after closure [15]. Adopting the best practice involves a number of risks and obstacles driven by the community, geographic, and climatic elements as well as government policies and regulatory frameworks. The best practice does not consist of a single answer that includes alternatives for disposal, long-term storage, filtration, and re-use. The red mud used in the analysis was collected from Belagavi, India's HINDALCO Aluminum refinery. In order to get the fine type of powder, raw red mud granules are ball-milled and sieved to different sizes. For the reinforcement, an average size of 90µm was chosen. Gravimetric testing confirms the existence of many elements, including aluminum, iron, silica, calcium, and titanium, as well as a variety of minor ingredients, including Cr, Na, Ba, Cu, K, Zn, V, Ni, Mn, Pb, etc. Some of the significant elements and their weight percentages are listed in Table 1. The density of the red mud is in the range of 3.2 g/cm$^3$. Figure 2 demonstrates the SEM micrograph of the red mud powder.

Table 1. Chemical composition of red mud

| Element | Content (%) |
|---|---|
| LOI | 8.00 |
| CaO | 1.00 |
| $Na_2O$ | 3.42 |
| $TiO_2$ | 9.56 |
| $SiO_2$ | 7.23 |
| $Fe_2O_3$ | 45.93 |
| $Al_2O_3$ | 18.34 |
| Etc. | 6.52 |

### 2.3 Casting and Testing.

Compared to alternative fabrication methods, a traditional stir casting procedure is the best method for processing AMCs [7–13]. In order to remove the trapped gases inside the melt, C2Cl6 - solid hexachloroethane was added. To make sure the degassing agent was properly mixed into the melt, stirring was done for five minutes at a speed of 50 rpm. The metal was finally separated from the slag. In an electrical resistance furnace, the Al-8011 alloy was melted at 750 °C. The warmed reinforcement particles with a wetting agent Mg [9,26] were injected into the vortex at a temperature of 700 0C with varied weight percentages. After adding the reinforcement and wetting agent to the melt, mechanical stirring at 150 rpm for 10 minutes was done to make sure there was appropriate mixing and uniform dispersion of the particles in the matrix alloy. The mixture is then kept in the furnace until it reaches the required pouring temperature. To lessen ambient contamination, cover flux (NaCl 45% + KCl 45% + NaF 10%) was applied to the molten metal before being poured into the mold.

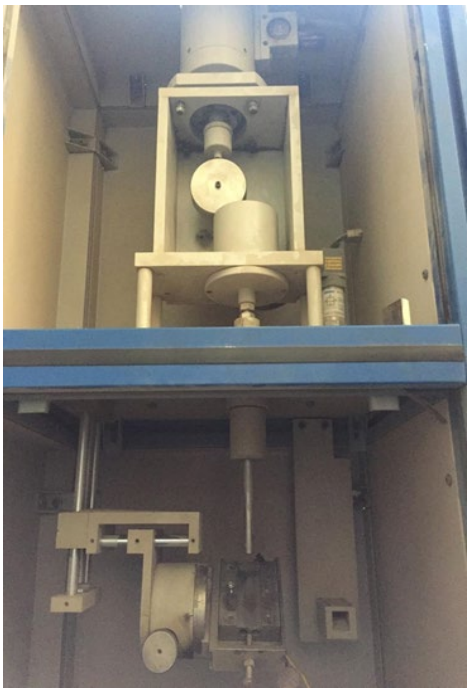

(a)

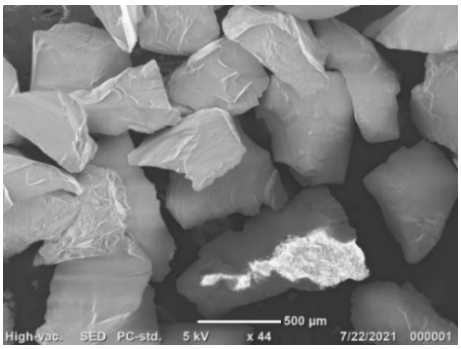


(b)

**Fig. 3:** (a) Air jet erosion test rig and (b) SEM of Silica particles

The casted specimens are then machined accordance with ASTM G76 standards. A high precision electronic weighing machine of accuracy 0.0001mg was used to determine the weight of the composite specimens before and after the abrasive test. The impact of the erosion by the air jet solid particles on the composite specimens is quantified by the weight loss method. The feed rate of solid silica particles was controlled by varying the air flow rate, and the impinging rate was modified by varying the speed of the conveyor system that delivers the solid particles to the jet of air. Figure 3 (b) shows the SEM micrographs of the silica powder which is used as an erodent in air jet erosion testing equipment and shows the sharp edges and grainy distribution. It can be said that the material which undergoes frequent contact with these particles experience high level of damage due to the sharp edges. The air jet erosion test rig used in this study is shown in the figure 3 (a).

## 3. Design of Experiments

It's critical to correctly arrange the experiment so that the appropriate data type and sample size are accessible to answer the research questions as clearly and efficiently as feasible. Design of experiments (DOE) is a strategy for determining the relationships between the factors that affect a process and its outputs that is structured and organized. Conduct and analyse controlled trials to determine the factors that influence the value of one or more parameters. Compared to many other designs, the experimental design using orthogonal matrices is an efficient technique.

Table 2: Parameters and levels considered for testing

| **Control Factor** | **L-1** | **L- 2** | **L- 3** | **L- 4** | **L- 5** |
|---|---|---|---|---|---|
| Stand of Distance (SOD) in mm | 10 | 15 | 20 | 25 | 30 |
| Angle of impingement (AOI) in Degree | 15 | 30 | 45 | 60 | 90 |
| Time in Minutes | 3 | 6 | 9 | 12 | 15 |
| Composition of RMp in Wt. % | 0 | 2 | 4 | 6 | 8 |

Table 3: Physical layout of the experimentation

| **Sl. No.** | **Sample** | **SOD** | **AOI** | **Time** |
|---|---|---|---|---|
| 1 | Base alloy | 10 | 15 | 3 |
| 2 | Al-2%RMp | 10 | 30 | 6 |
| 3 | Al-4%RMp | 10 | 45 | 9 |
| 4 | Al-6%RMp | 10 | 60 | 12 |
| 5 | Al-8%RMp | 10 | 90 | 15 |
| 6 | Al-4%RMp | 15 | 15 | 6 |
| 7 | Al-6%RMp | 15 | 30 | 9 |
| 8 | Al-8%RMp | 15 | 45 | 12 |
| 9 | Base alloy | 15 | 60 | 15 |
| 10 | Al-2%RMp | 15 | 90 | 3 |
| 11 | Al-8%RMp | 20 | 15 | 9 |
| 12 | Base alloy | 20 | 30 | 12 |
| 13 | Al-2%RMp | 20 | 45 | 15 |
| 14 | Al-4%RMp | 20 | 60 | 3 |
| 15 | Al-6%RMp | 20 | 90 | 6 |
| 16 | Al-2%RMp | 25 | 15 | 12 |
| 17 | Al-4%RMp | 25 | 30 | 15 |
| 18 | Al-6%RMp | 25 | 45 | 3 |
| 19 | Al-8%RMp | 25 | 60 | 6 |
| 20 | Base alloy | 25 | 90 | 9 |
| 21 | Al-6%RMp | 30 | 15 | 15 |
| 22 | Al-8%RMp | 30 | 30 | 3 |
| 23 | Base alloy | 30 | 45 | 6 |
| 24 | Al-2%RMp | 30 | 60 | 9 |
| 25 | Al-4%RMp | 30 | 90 | 12 |

The minimum number of necessary experiments is determined by the Taguchi method, Table 2 identifies and lists the parameters that affect the mechanical properties and wear behaviour of composite materials. Given that there are 4 main factors and 5 levels in the current study, the total DOF is equal to (No of levels - 1) x No of Main factors (5 - 1) x 4= 16 without accounting for the interactions between the components. A minimum number of experiments is therefore equal to Total DOF + 1. Therefore, an appropriate OA is one that has an equivalent or higher number of experiments than DOF overall. Consequently, L25 OA was chosen, and Table 3 provides the physical setup of the experiment.

## 4. Results and Discussion

Figure 4 shows the EDX of Al-8011-4%RM. It can be seen that the presence of different elements like iron, silica, aluminum, and chromium as well as an array of other

atoms of Zn, Cu, C, Mn etc, thus EDX analysis confirms the presence of red mud particles in the composites prepared. Figure 5 shows the worn surfaces of the Al-RMp composites. As many researches states that the addition of reinforcement in the ductile materials leads to brittle transition the same trend was observed in the tested composites. The ductile deformed spikes were observed in the figure 5 (a), as it contains only 2% of RMp the ductility in the matrix alloys remains. From the figure 5 (b), (c) and (d) it's clear that the ductility is compromised with the addition of RMp in a higher percentage, thus lead the composite materials harder and wear resistant.

The purpose of a wear test is to identify the important components, their relationships, and their optimum values in order to obtain the lowest wear rate possible. In compared to the Al- RMp composites the matrix Alloy shows more wear, as shown by the numbers in Table 4. This could be because red mud particles function as a solid hard particle between the composite and the rubbing surface. As the amount of red mud goes from 0% to 8%, the rate of wear reduces.

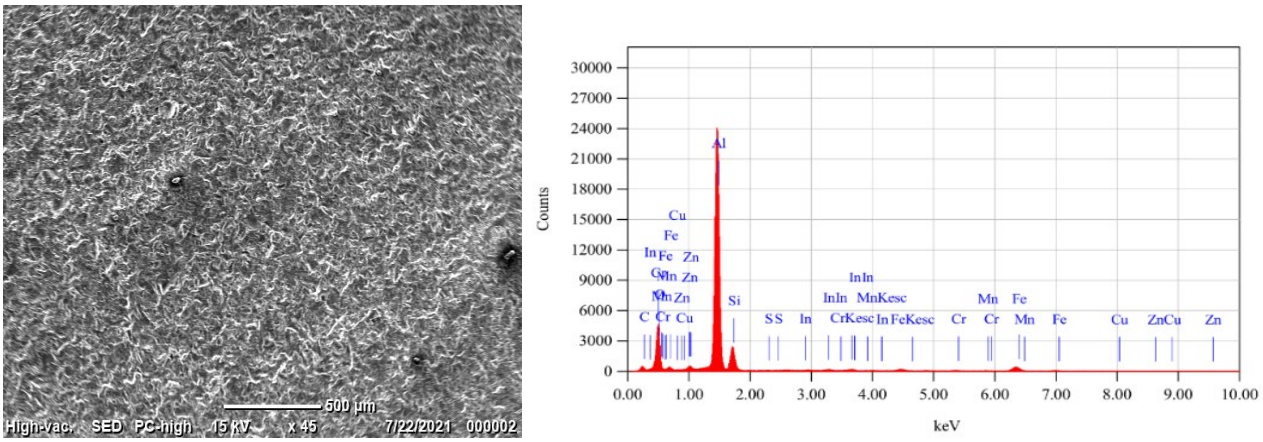


**Fig. 4:** EDX analysis of Al-RMp Composite.

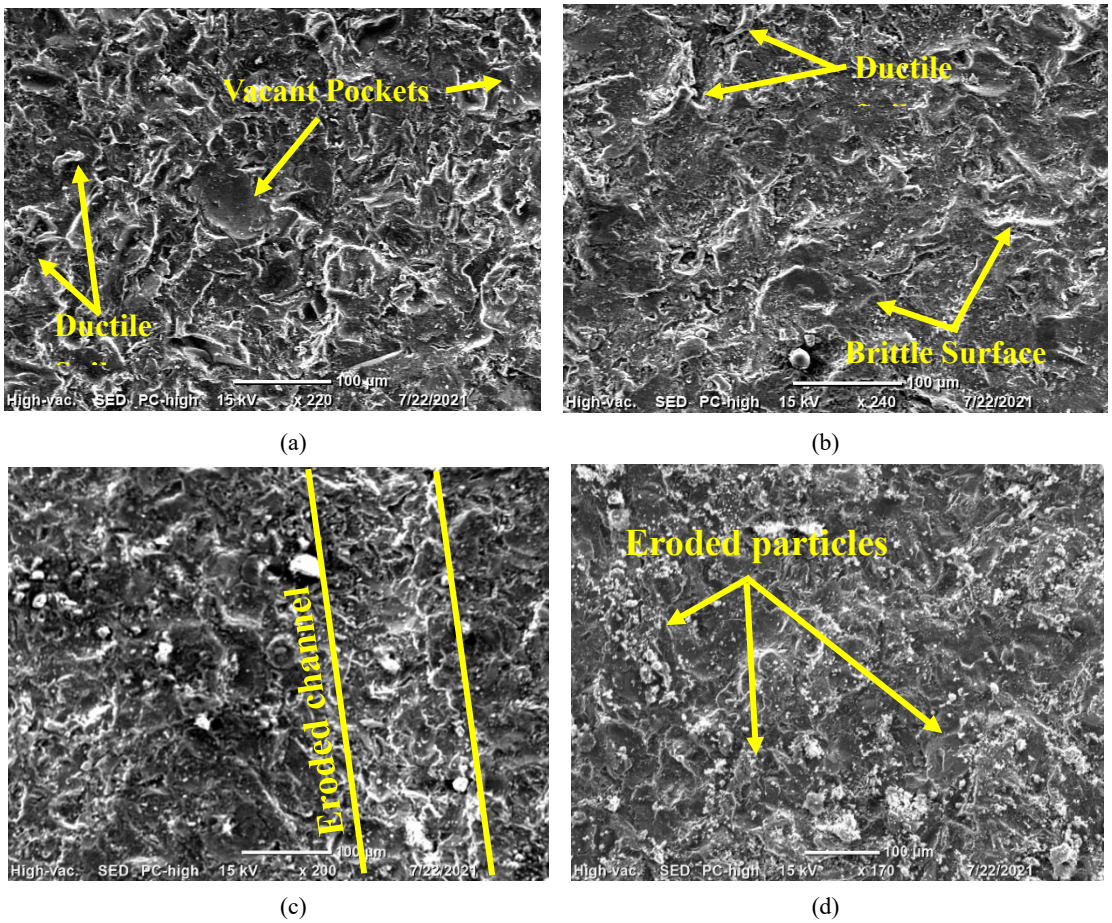


**Fig. 5:** SEM micrographs of eroded specimens (a) Al-2%RMp, (b) Al-4%RMp, (c) Al-6%RMp, and (d) Al-8%RMp.

Taguchi's Technique was used to conduct the trials. The L25 orthogonal array was used, and 25 tests were carried out according to the physical architecture of the experimentation shown in Table 3. The wear rate results are provided in table 4, which was evaluated using the software MINITAB V.19.1. The Signal to Noise Ratio (SNR) for weight loss achieved from each trial is shown in Table 5. The rank values indicate how much input factors influence the response variable. Thus, composition had the greatest influence on weight loss, followed by Time, SOD, and AOI, which may be due to some experimental noise and the complexity of the experimental design. The same is reflected in % in the last column of table 6 ANOVA findings. The ANOVA table's P-value identifies the variables that significantly affect weight loss. Because their P-values are less than 0.05, SOD, Time, and comp. are significant factors affecting wt. Loss, but AOI has no effect on the response parameter wt. Loss.

Note: DF stands for Degree of Freedom; Adj SS stands for Adjusted Sum of Squares; Adj MS stands for Adjusted Mean Squares; and P stands for Percentage Contribution. The degree of fit is measured by the R2 value. The fitted model fits the actual data better as the R2 value approaches unity. It also indicates how much uncontrollable factors influence performance qualities. The current R2 score can explain 78.25 percent of data variability. As a result, it is confirmed that the current model adequately explains the link between the input variables and the response variable. The relationship between two or more input variables and one response variable is modelled using linear multiple regression analysis. It tries to fit observed data into a linear regression equation. The wear loss multiple regression equation is given in Eq-1.

Weight loss = 0.6003 - 0.00509 SOD - 0.000136 AOI + 0.01147 Time - 0.02878 Comp----------(1)

Table 4: Air jet erosion test results with computed S/N ratio

| SOD | AOI | Time | Comp. of RMp | Wt. loss (gram) | SNRA1 |
|---|---|---|---|---|---|
| 10 | 15 | 3 | 0 | 0.535 | 5.432924 |
| 10 | 30 | 6 | 2 | 0.576 | 4.79155 |
| 10 | 45 | 9 | 4 | 0.541 | 5.336055 |
| 10 | 60 | 12 | 6 | 0.454 | 6.858883 |
| 10 | 90 | 15 | 8 | 0.458 | 6.78269 |
| 15 | 15 | 6 | 4 | 0.521 | 5.663246 |
| 15 | 30 | 9 | 6 | 0.369 | 8.659473 |
| 15 | 45 | 12 | 8 | 0.43 | 7.330631 |
| 15 | 60 | 15 | 0 | 0.788 | 2.069476 |
| 15 | 90 | 3 | 2 | 0.48 | 6.375175 |
| 20 | 15 | 9 | 8 | 0.4301 | 7.328611 |
| 20 | 30 | 12 | 0 | 0.708 | 2.999335 |
| 20 | 45 | 15 | 2 | 0.639 | 3.889983 |
| 20 | 60 | 3 | 4 | 0.398 | 8.002339 |
| 20 | 90 | 6 | 6 | 0.344 | 9.268831 |
| 25 | 15 | 12 | 2 | 0.401 | 7.937113 |
| 25 | 30 | 15 | 4 | 0.502 | 5.985926 |
| 25 | 45 | 3 | 6 | 0.355 | 8.995433 |
| 25 | 60 | 6 | 8 | 0.38 | 8.404328 |
| 25 | 90 | 9 | 0 | 0.58 | 4.73144 |
| 30 | 15 | 15 | 6 | 0.459 | 6.763746 |
| 30 | 30 | 3 | 8 | 0.265 | 11.53508 |
| 30 | 45 | 6 | 0 | 0.523 | 5.629966 |
| 30 | 60 | 9 | 2 | 0.421 | 7.514358 |
| 30 | 90 | 12 | 4 | 0.445 | 7.0328 |

Eq-1 can be used to estimate the Al8011-red mud composite's wear loss. Eq-1 has a negative coefficient of weight percent, indicating that as weight percent increases, wear rate decreases. SOD and AOI have a negative effect on wear loss because they cause metal to erode. The figure 6 shows effect of stand of distance on wear rate, which is decreasing as the distance of nozzle is increased from test sample. The highest wear is noticed when stand of distance is at 10 mm and gradually decreases from there as we move to 30 mm. This is understandable because the erodent particles will lose their kinetic energy as they move in air for longer distance and hit the sample specimen. In addition to this, the higher standoff distance means the erodent particles are more likely to get dispersed. As shown in these data, weight loss for the matrix material and composites increases with increasing angle of impingement up to 45°, then reduces with increasing angle of impingement for a specific standoff distance and testing period.

Both the matrix material and the produced composites had maximum wear at 45°, and at 15° and 90° impinging angle, the wear mass loss is the smallest. The formation of abrasion grooves is mostly responsible for material removal at lower angles of impingement. This is because the impinging silica sand particles are more likely to move across the target surface at a lower angle of impingement, generating more abrasion grooves and causing less material loss due to abrasion groove development, resulting in a lower erosive wear rate. At a lower angle of impingement, the depression is shallower and longer. The

removal of material at 45°, on the other hand, is mostly owing to strong indentation, brittle fracture, and increased crater development.

Table 5: Signal to Noise Ratio Response Table
(Smaller is better)

| Level | SOD | AOI | Time | COMP |
|---|---|---|---|---|
| 1 | 5.840 | 6.625 | 8.068 | 4.173 |
| 2 | 6.020 | 6.794 | 6.752 | 6.102 |
| 3 | 6.298 | 6.236 | 6.714 | 6.404 |
| 4 | 7.211 | 6.570 | 6.432 | 8.109 |
| 5 | 7.695 | 6.838 | 5.098 | 8.276 |
| Delta | 1.855 | 0.602 | 2.970 | 4.104 |
| Rank | 3 | 4 | 2 | 1 |

The weight loss of the samples increases linearly as the testing time for a specific impinging angle, standoff distance, and testing time for the generated cold cast matrix and composites increases. This is because when silica sand hard erodent particles collide with the exposed target surface of the specimen, the kinetic energy and momentum of the impinging hard erodent particles are transferred to the exposed surface during the erosion phenomenon, resulting in material removal from the exposed target surface. The figure 6 also shows that when the weight % of reinforcement increases, the wear rate lowers gradually until it reaches a certain level. With increasing wt. % it drastically drops after that point. However, the difference in slopes between the two halves of the graph is not significant. With an increase in weight, the wear rate falls significantly in the first section and slightly in the remaining part over time. As a result, the best values for minimum wear rate are 8% of red mud weight, 30 mm distance and 15°- or 90°-degree angle. The major effects plot for the S/N ratio for wear rate vs. all input parameters is shown in figure 7. Because a lower minimum wear rate is desirable, the best alternative was chosen. The S/N ratio graph shows that with 8% red mud, 30 mm or distance, 15 degrees of angle of impingement and 3 minutes of time, the least wear rate is attained.

Table 6: Analysis of variance

| Source | DF | Adj SS | Adj MS | F-Value | P-Value |
|---|---|---|---|---|---|
| SOD | 1 | 0.032360 | 0.032360 | 9.04 | 0.007 |
| AOI | 1 | 0.000307 | 0.000307 | 0.09 | 0.773 |
| Time | 1 | 0.059168 | 0.059168 | 16.54 | 0.001 |
| COMP | 1 | 0.165635 | 0.165635 | 46.29 | 0.000 |
| Error | 20 | 0.071565 | 0.003578 | | |
| Total | 24 | 0.329034 | | | |

Table 7: Summary of model

| R-sq | R-sq(adj) |
|---|---|
| 78.25% | 73.90% |

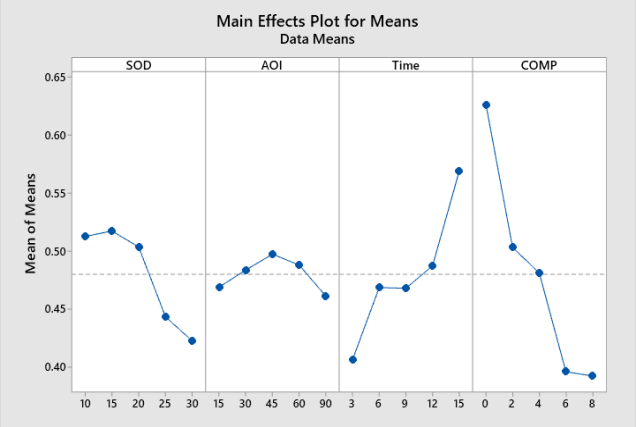


**Fig. 6**: Main Effect Plot for Means

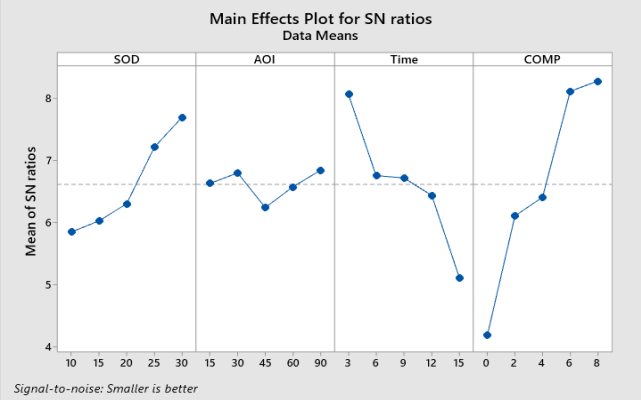


**Fig. 7:** Main Effect Plot for signal to noise ratio

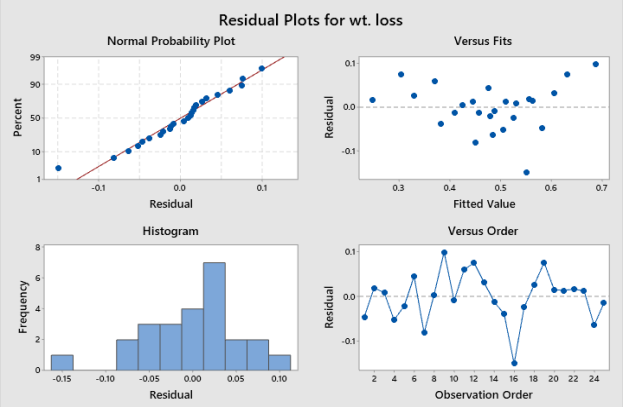


**Fig. 8**: Four in one regression charts

Most Residuals follow the straight line in the Normal Probability Plot, as shown in figure 8 whereas others are closer to it. This result demonstrates that the normalcy assumption is upheld. The right and left tails are equal in this graph. The patterns in the dots in Residual v/s Fitted

Value Plot could imply that residuals close together are connected and thus not independent. In our case, independent residuals are displayed in temporal order but do not exhibit any trends or patterns. The spots on the residual versus fits plot are dispersed at random. Except for one outlier that has dropped below -0.1, none of the groups seem to have significantly different variability.

## 5. Conclusion

The purpose of the current study is to enhance the tribological performance of a composite material consisting of Al 8011 and Red mud, which was manufactured using conventional stir casting. An erosion test was carried out using an air jet erosion tester with L25 Taguchi array DOE. The findings of the study are summarized as follows:

- Al 8011-Red mud MMC can be satisfactorily synthesize using a stir casting process by varying the reinforcement percentage. This is because micrograph of Graphite with Al 8011 metal matrix composite reveals a reasonably consistent distribution of reinforcements.
- As the composition of red mud in wt. percentage is increased, the composite has positive effect of weight loss. In our experiment minimum weight loss was observed at 8% red mud addition.
- Minitab was used to successfully analyses and visualizes the collected data and steps of doing so were also documented.
- The effect of parameters like red mud weight percentage, AOI, SOD and time, and their relation in weight loss during air jet erosion was established and modelled using regression analysis.
- The Al-8% RMp composite specimen showed the least amount of wear when tested for 3 minutes at an AOI of 15 and 90 degrees and a normal load of 30 mm SOD.

### References


1) Sanman, S., and Sreenivas Rao, K V. “Influence of Reinforcement Particulate Size and Weight Fraction on the Wear Properties of Chill Cast Al-B4C Composites”, International Journal of Applied Engineering Research ISSN 0973-4562, 10, pp 10292-10295 (2015).
2) Xavier, L.F., and Suresh, P. “Wear behavior of aluminum metal matrix composite prepared from industrial waste”, The Scientific World Journal, 2, pp 1–9. (2016) Doi:10.1155/2016/6538345.
3) Kumaraswamy, J., Vijaya Kumar and Purushotham, G. “A review on mechanical and wear properties of ASTM a 494 M grade nickel-based alloy metal matrix composites”, Materials Today: Proceedings, 37, pp 2027–2032. (2021) Doi: 10.1016/j.matpr.2020.07. 499.
4) Karthikkumar, C., Baranirajan, R., Premnauth, I., and Manimaran, P. “Investigations on Mechanical properties of AL 8011 reinforced with micro B4C / Red Mud by Stir Casting Method”, International Journal of Engineering Research and General Science, 4 (2), PP-405-412. (2016).
5) Shaik Mujeeb Quader, Suryanarayana Murthy, B., and Pinninti Ravinder Reddy. “Processing and Mechanical Properties of Al2O3 and Red Mud Particle Reinforced AA6061 Hybrid Composites”, Journal of Minerals and Materials Characterization and Engineering, 4, pp 135-142 (2016).
6) Jayappa, K., Kumar, V. and Purushotham, G. “Effect of reinforcements on mechanical properties of nickel alloy hybrid metal matrix composites processed by sand mold technique”, Applied Science and Engineering Progress, 14(1), pp. 44–51. (2021). DOI: 10.14416/j.asep.2020.11.001.
7) Campbell. “Manufacturing technology for aerospace structural materials”, Butterworth- Heinemann publications, ISBN: 978-1-85-617495-4, Elsevier Inc. (2006).
8) U.S. Geological Survey, Mineral Commodity Summaries, Jan 2020. https://pubs.usgs.gov/periodicals/mcs2020/mcs2020.pdf
9) Rana, R. S., Rajesh Purohit, and Das, S. “Review of recent Studies in Al matrix composites”, International Journal of Scientific & Engineering Research, 3(6). (2012).
10) Bhaskar, H.B, and Abdul sharief. “Tribological Properties of Aluminium 2024 Alloy–Beryl Particulate MMC’s”, Bonfring International Journal of Industrial Engineering and Management Science, 2 (4), pp 143-147. (2012)
11) Reddappa, H. N., Suresh, K. R., Niranjan, H. B, and Satyanarayana, K. G. “Effect of Aging on Mechanical and Wear Properties of Beryl Particulate Reinforced Metal Matrix Composites”, Journal of Engineering Science and Technology, 9(4), pp 455-462. (2014).
12) Jayappa, K., Kumar, V. and Purushotham, G. “Thermal analysis of nickel alloy/Al2O3/TiO2 hybrid metal matrix composite in automotive engine exhaust valve using FEA method”, Journal of Thermal Engineering, 7(3), pp. 415-428. (2021). Doi: 10. 18186/thermal.882965.
13) Radhika, N., Subramanian, R, and Venkat Prasat, S. “Tribological Behaviour of Aluminium/Alumina/ Graphite Hybrid Metal Matrix Composite Using Taguchi’s Techniques”, Journal of Minerals & Materials Characterization & Engineering, 10(5), pp. 427-443. (2011).
14) Sujan, D., Oo, Z., Rahman, M.E., Maleque, M.A, and. Tan, C.K. “Physio-mechanical Properties of Aluminium Metal Matrix Composites Reinforced with Al2O3 and SiC”, International Journal of

Engineering and Applied Sciences, 6, pp- 288-291. (2012).
15) Davis, J.R. Aluminum and Aluminum Alloys, ASM International, pp 351-416, Doi:10.1361/autb2001 p351.
16) Kumaraswamy, J., Vijaya Kumar and Purushotham, G. "Evaluation of the microstructure and thermal properties of (ASTM A 494 M grade) nickel alloy hybrid metal matrix composites processed by sand mold casting", International Journal of Ambient Energy,42, pp. 1-10. (2021). DOI:10.1080/01430750. 2021.1927836.
17) Rahimi, M., Fojan, P., Gurevich, L, and Afshari, A. "Aluminium alloy 8011: Surface characteristics", Applied Mechanics and Materials, 719-720, pp 29-37.
18) Valmir Martins Monteiro, Saulo Brinco Diniz, Bruna Godoi Meirelles, Luis Celso da Silva, Andersan dos Santos Paula. "Microstructural and Mechanical Study of Aluminium Alloys Submitted To Distinct Soaking Times During Solution Heat Treatment", Tecnol. Metal. Mater. Miner., São Paulo, 11(4), pp 332-339. (2014). Doi: /10.4322/tmm.2014.047.
19) Marek, J., Karlík, M., Sláma, P.. "Textures of Aluminum Alloy Thin Sheets for Heat Exchanger Fins", Materials Structure, 8 (1), Pp 25-28. (2001)
20) Bauxite residue management: best practice, international aluminum Institute (IAI). (2015). www. World-aluminum.org.
21) Sreenivasrao, K. V., Anil, K. C., Girish, K. G. and Akash. "Mechanical characterization of red mud reinforced Al-8011 matrix composite", ARPN Journal of Engineering and Applied Sciences, 11(1), pp-229-234. (2016)
22) Anil, K.C., Sachin Gadge, Rishabh Kumar Srivastva and Sreenivas Rao, K.V. "Three-Body Abrasive Wear Behavior of Al-8011 alloy Reinforced with Graphite and Red Mud Particulates", International Journal of Science, Engineering and Management (IJSEM), 2 (2), pp-29-33. (2017).
23) Anil, K.C., Vikas, M.G., Shanmukha Teja, B. and Sreenivas Rao, K.V. "Effect of cutting parameters on surface finish and machinability of graphite reinforced Al-8011matrix composite", Materials Science and Engineering, 191(012025). (2017). DOI:10.1088/1757-899X/191/1/012025
24) Sreenivas Rao, K.V., Anil, K.C., Akash and Girisha, K. G. "Effect of Particle Size on Mechanical Properties of Al-RMp Metal Matrix Composites", Materials Today: Proceedings, Science Direct pp-11154–11157. (2017). DOI: 10.1016/j.matpr.2017. 08.080
25) Harshavardhan, R., Anil, K.C. and Sreenivas Rao, K.V. "Evaluation of Fracture Toughness of Red Mud Reinforced Aluminium Matrix Composite, Materials" Today: Proceedings, 5, pp 24854–24861. (2018) DOI: 10.1016/j.matpr.2018.10.284.
26) Anil, K.C., Kumaraswamy, J., Akash, and Sanman, S. "Experimental arrangement for estimation of metal-mold boundary heat flux during gravity chill casting", Materials Today: Proceedings, (2022) Doi: 10.1016/ j.matpr.2022.07.399.
27) H. Sosiati, N.D.M. Yuniar, D. Saputra, and S. Hamdan, "The Influence of Carbon Fiber Content on the Tensile, Flexural, and Thermal Properties of the Sisal/PMMA Composites" EVERGREEN Joint Journal of Novel Carbon Resource Sciences & Green Asia Strategy, Vol. 09, Issue 01, pp32-40, (2022), doi.org/10.5109/4774214.
28) Anthony Chukwunonso Opia1, Mohd Kameil Abdul Hamid, Samion Syahrullail, Audu Ibrahim Ali, Charles N. Johnson, Ibham Veza, Mazali Izhari Izmi, Che Daud Zul Hilmi, Abu Bakar Abd Rahim, "Tribological Behavior of Organic Anti-Wear and Friction Reducing Additive of ZDDP under Sliding Condition: Synergism and Antagonism Effect" EVERGREEN Joint Journal of Novel Carbon Resource Sciences & Green Asia Strategy, Vol. 09, Issue 02, pp246-253, (2022), doi.org/10.5109/ 4793628.
29) Muhammad Miqdad, Anne Zulfia Syahrial, "Effect of Nano Al2O3 Addition and T6 Heat Treatment on Characteristics of AA 7075 / Al2O3 Composite Fabricated by Squeeze Casting Method for Ballistic Application" EVERGREEN Joint Journal of Novel Carbon Resource Sciences & Green Asia Strategy, Vol. 09, Issue 02, pp531-537, (2022). doi.org/10.5109 /4794184.
30) Mr. Dilip Choudhari, Dr. Vyasraj Kakhandki, "Characterization and Analysis of Mechanical Properties of Short Carbon Fiber Reinforced Polyamide66 Composites" EVERGREEN Joint Journal of Novel Carbon Resource Sciences & Green Asia Strategy, Vol. 08, Issue 04, pp768-776, (2021). doi.org/10.5109/4742120.
31) Anthony Chukwunonso Opia, Mohd Kamei Abdul Hamid, Samion, Syahrullail, Charles A. N. Johnson, Abu Bakar Rahim, Mohammed B. Abdulrahman, " Nano-Particles Additives as a Promising Trend in Tribology: A Review on their Fundamentals and Mechanisms on Friction and Wear Reduction" EVERGREEN Joint Journal of Novel Carbon Resource Sciences & Green Asia Strategy, Vol. 08, Issue 04, pp777-798, (2021). doi.org/10.5109/ 4742121.